# Electrostatic Potential and Free Energy of Proteins: A Comparison of the Poisson−Boltzmann and the Bogolyubov−Born−Green−Yvon Equations

**Sergei Gavryushov* and Piotr Zielenkiewicz**

*Institute of Biochemistry and Biophysics, Polish Academy of Sciences, Pawinskiego 5a, 02-106 Warszawa, Poland*

*Received: May 7, 1997; In Final Form: August 1, 1997*[⊗]

The Bogolyubov−Born−Green−Yvon (BBGY) equations have been applied to study ionic and mean electrostatic potential distributions around a macromolecule of arbitrary shape and charge distribution. Results for the lysozyme molecule are compared with those obtained by classical Poisson−Boltzmann (PB) calculations. It is found that ion−image charge interactions and interionic correlations which are neglected by the PB equation have a weak effect on the electrostatic potential near charged groups of the protein, but they notably change electrostatic potential and ionic atmosphere at significant separation from the macromolecule. It is also shown that even for diluted solutions of electrolyte only a part of the observed macromolecule's free energy dependence on salt concentration might originate from long-range electrostatic forces. The rest comes from polarization forces within a very thin shell (∼2 Å) around the macromolecule's surface, where macroscopic description of electrostatics cannot be used.

## 1. Introduction

It is well-known that salt-dependent electrostatic effects are an important contributor to solvation and binding energies of charged macromolecules such as nucleic acids and proteins. It is also known that despite dramatic progress in Monte Carlo or molecular dynamics simulations, serious problems remain in the microscopic description of phenomena involving Coulombic forces. The large number of solvent molecules and effects of free ions within the solvent make the microscopic approaches practically impossible to serve the purpose.

An alternative approach based on continuum description of dielectric properties of macromolecules and solvent is the PB equation, which can be solved for enough realistic structural models of proteins[1−4] and DNA.[5] At present this is the only method that allows the study of salt dependence effects on the free energy of a macromolecule[6,7] and its charged groups of atoms[8] if we want to take into account both the geometry of the macromolecule and the difference between dielectric properties of the macromolecule and solvent. An advantage of the method is that the contribution of these parameters is significant to the salt dependence of binding free energy.[9]

Despite the obvious success of the PB equation for many biological systems, it should be noted that this equation is the simplest form of the statistical mechanical theory of the electrical double layer within the framework of the continuum solvent model.[10] The equation ignores the finite size of solvent ions and spatial correlations between them, which reduces the range of salt concentrations over which it can be applied to diluted solutions. It also neglects repulsion between ions and their image charges produced in the cavity of low dielectric constant representing a macromolecule.[10]

The PB equation was checked by Monte Carlo simulations and hypernetted chain (HNC) calculations,[11−13] where discrete ion effects can be included explicitly. The comparisons of solutions showed that for multivalent electrolytes the PB equation can produce large errors even at low ionic concentrations. The PB equation was also compared with Monte Carlo simulations in the case of a more realistic model of DNA[14] but only for monovalent electrolyte and without image interactions of ions. The comparisons have not been extended to account for the shape, charge distribution, and dielectric properties for realistic models of other macromolecules, so true errors due to neglecting the finite size of ions and interionic correlations remain uncertain. Elimination of image forces leads to a more serious problem. These forces take part in such phenomena as increase of surface tension of electrolyte solutions[10] and salting-out of proteins.[15] As follows from protein solubility data,[15−18] salting-out effects can be a major contributor to the protein free energy dependence on salt concentration even at moderate dilution of electrolyte (less than ∼0.5 M). The role of long-range electrostatic forces in this phenomenon is still unclear.

The use of the continuum solvent model (McMillan−Mayer level of description) raises questions as well. As follows from recent works studying three-component systems,[19−21] driving forces of solvent drastically affect ionic distributions, making them essentially oscillatory near smooth surfaces. The solvent structure is affected very little by even a high external electric field. In the present paper we do not consider such effects and concentrate on simplifications, outlined above, i.e. on interionic correlations and image interactions. The restricted primitive model (RPM) is used throughout the paper for description of short-range interactions between ions. In other words, ions are represented by charged hard spheres immersed in a continuous medium.

The present work makes a comparison of PB calculations with the more advanced BBGY approach for a protein molecule of complex form and charge distribution. The BBGY equations are an exact formalism which can be applied to the electrical double layer. Being supplemented by a suitable closure approximation, these equations allow the effects of the finite size of ions and image forces to be incorporated into the theory. Such an approach was initially implemented in the modified Poisson−Boltzmann (MPB) theory developed through the years.[22−26] The basis of the MPB theory is the Kirkwood or BBGY hierarchy of equations together with linearized Loeb's closure ("weak ion−ion coupling") for the RPM.[10] The MPB

* Corresponding author. Tel: 48 2 6584703. Fax: 48 39 121623. E-mail: serg@ibbrain.ibb.waw.pl.

⊗ Abstract published in *Advance ACS Abstracts,* November 15, 1997.

S1089-5647(97)01536-8 CCC: $14.00 

equations based on the Kirkwood−Loeb approach were formulated for the planar, spherical, and cylindrical geometries.[23−25] The MPB equation based on the BBGY hierarchy was derived for the planar geometry.[26] These applications were designed for approximate solutions of the electrostatic boundary value problems, which can only be done for the simplest geometries. In our research the same closure is applied to the BBGY hierarchy of equations, and all electrostatic boundary value problems are solved numerically. The last allows the mean electrostatic potential and ionic distributions to be obtained for an arbitrarily complex macromolecule. The method has been previously tested on the data of the Monte Carlo simulations for the cylindrical polyion.[27] In the present work it was extended to a macromolecule described in terms of its three-dimensional structure and detailed charge distribution. All the partial differential equations are now solved as three-dimensional equations. The algorithm was tested on uniformly charged spherical models, where numerical solution can be independently obtained by the Runge−Kutta method.

We concentrate our efforts on calculations of the macromolecule's free energy dependence on concentration of electrolytes. The molecule of hen egg lysozyme was taken as an example. An advantage of this choice is that the molecule is not too highly charged and not too large and data of its solvation free energy for various electrolytes are present in the literature. Comparison of results given by BBGY and PB calculations was carried out. The main subject of our interest was the effect of locally intensive electric field near charged groups of the protein and the influence of image forces on resulting electrostatic potential and free energy of the molecule in solution.

## 2. Theory

The BBGY hierarchy together with linearized Loeb's closure gives the following equations for distribution of ions of species $\alpha$, represented by hard spheres of diameter $d$:[10]

$$\ln g_\alpha(\mathbf{r}) = \ln \xi_\alpha(\mathbf{r}) - \beta q_\alpha \psi(\mathbf{r}) - \beta q_\alpha \{\eta_\alpha(\mathbf{r}) - \eta_\alpha(\infty)\} \quad (1)$$

where $\beta = 1/kT$, $q_\alpha$ is the charge of an ion, $\psi(\mathbf{r})$ is the mean electrostatic potential, $-kT \ln \xi_\alpha(\mathbf{r})$ is the work required to insert an uncharged ion at point $\mathbf{r}$, and $\eta_\alpha(\mathbf{r})$ satisfies the equation

$$\nabla_2 \eta_\alpha(\mathbf{r}_2) = \lim_{\mathbf{r}_1 \to \mathbf{r}_2} \nabla_1 [\phi_\alpha(\mathbf{r}_1,\mathbf{r}_2) - q_\alpha u^C(r_{12})] \quad (2)$$

where $q_\alpha u^c(r_{12})$ is Coulombic self-potential of the ion and $\phi_\alpha(\mathbf{r}_1,\mathbf{r}_2)$ is the fluctuation potential. The last satisfies the partial differential equations for the RPM:

$$\nabla_1^2 \phi_\alpha(\mathbf{r}_1,\mathbf{r}_2) = 0 \quad (3.1)$$

(inside the macromolecule's interior and a shell of thickness $d/2$ surrounding the surface of the macromolecule),

$$\nabla_1^2 \phi_\alpha(\mathbf{r}_1,\mathbf{r}_2) = -\nabla_1^2 \psi(\mathbf{r}_1) - \frac{4\pi}{\epsilon_w} q_\alpha \delta(\mathbf{r}_1 - \mathbf{r}_2) \quad (3.2)$$

(outside the macromolecule and the "$d/2$ shell", $r_{12} < d$),

$$\nabla_1^2 \phi_\alpha(\mathbf{r}_1,\mathbf{r}_2) = k^2(\mathbf{r}_1)\, \phi_\alpha(\mathbf{r}_1,\mathbf{r}_2) \quad (3.3)$$

(outside the macromolecule and the "$d/2$ shell", $r_{12} > d$), where

$$k^2(\mathbf{r}) = (4\pi\beta/\epsilon_w) \sum_\gamma n_\gamma(\mathbf{r}) q_\gamma^2$$

$n_\gamma(\mathbf{r}) = n_\gamma^0 g_\gamma(\mathbf{r})$ and $n_\gamma^0$ are the mean ionic concentration and the bulk ionic concentration, respectively.

Equations 3.1−3.3 are subject to the boundary conditions on the surface of the macromolecule:

$$\phi_\alpha|_{\text{inside}} = \phi_\alpha|_{\text{outside}}$$

$$\epsilon \frac{\partial \phi_\alpha}{\partial n}\Big|_{\text{inside}} = \epsilon_w \frac{\partial \phi_\alpha}{\partial n}\Big|_{\text{outside}} \quad (4)$$

where $\epsilon$ and $\epsilon_w$ are dielectric constants of the macromolecule's interior and water, respectively. The mean electrostatic potential $\psi(\mathbf{r})$ from (1) satisfies Poisson's equation:

$$\nabla^2 \psi(\mathbf{r}) = -\frac{4\pi}{\epsilon} \rho_0(\mathbf{r}) \quad \text{inside the macromolecule}$$

$$\nabla^2 \psi(\mathbf{r}) = -\frac{4\pi}{\epsilon_w} \sum_\gamma q_\gamma n_\gamma^0 g_\gamma(\mathbf{r}) \quad \text{outside the macromolecule} \quad (5)$$

where $\rho_0$ is the charge density of the macromolecule. As for the fluctuation potential, the boundary conditions for $\psi(\mathbf{r})$ on the macromolecule's surface require continuous $\psi$ and its normal derivative multiplied by the dielectric constant of the medium. At low ionic concentrations, the so-called exclusion volume term may be approximated by[28] $-\int_{V_\alpha} \sum_\gamma (n_\gamma(\mathbf{r}) - n_\gamma^0)\, dV$, where $V_\alpha = {}^4/_3\pi d^3$ is the excluded volume of a small ion of diameter $d$.

Neglecting the first and third terms of the right part of eq 1 and its substitution into eq 5 simplify eq 5 to the PB equation. Its solution gives initial $\psi^{(0)}(\mathbf{r})$, which makes it possible to obtain $\phi_\alpha^{(0)}(\mathbf{r}_1,\mathbf{r}_2)$ through eq 3; then one obtains $g_\alpha^{(1)}(\mathbf{r})$ through eq 1 and $\psi^{(1)}(\mathbf{r})$ through eq 5 and so on. This procedure was applied to a highly charged cylindrical polyion where a very fast convergence of loop (5)−(3)−(1)−(5) was observed.[27]

The electrostatic energy of a molecule can be obtained via two consequent processes: transfer of the uncharged macromolecule into electrolyte solution and charging up the macromolecule.

$$W(C_{\text{Salt}}) = W_0(C_{\text{Salt}}) + W_{\text{Ch}}(C_{\text{Salt}}) \quad (6)$$

The second term is

$$W_{\text{Ch}} = \int_0^1 d\lambda \int d^3\mathbf{r}\, \rho_0(\mathbf{r})\, \psi(\mathbf{r},\lambda) \quad (7)$$

and requires the solution of the BBGY equations at each charging state $\lambda$. The first term is expressed through the work of "ionic gas pressing":

$$W_0 = kT \sum_\gamma \int (n_\gamma^0 - n_\gamma(\mathbf{r}))\, d^3\mathbf{r} \quad (8)$$

where $n_\gamma(\mathbf{r})$ are obtained from system (1)−(5) at $\rho_0 = 0$. For the PB equation the $W_0$ term is obviously equal to zero and the second charging integral can be replaced by the energy-density integral,[6,7] which requires the PB equation to be solved only at the fully charged state $\lambda = 1$. Unfortunately, the method of computation of eq 6 cannot be simplified in such a manner for the BBGY equations.

Finally, one can write a change of the macromolecule free energy, or chemical potential, at its transfer from pure water into electrolyte solution:

$$\Delta\mu(C_{\text{Salt}}) = W(C_{\text{Salt}}) - W_{\text{Ch}}(0) \quad (9)$$

where $W_{\text{Ch}}(0) = {}^1/_2 \int d^3\mathbf{r}\, \rho_0(\mathbf{r})\, \psi(\mathbf{r})$; that is, the electrostatic

energy of a charged macromolecule in pure water and $\psi(\mathbf{r})$ is a corresponding solution of Poisson's equation.

## 3. Method

The PB equation has been widely used mostly due to the fact that it can be solved relatively easily. An attempt to implement numerically eqs 1−5 meets serious difficulties in the case of three-dimensional geometry. One of them is singularities in eqs 2 and 3.2. The second and main difficulty is a giant amount of computations because of the nature of eq 3. This equation has to be solved at all positions of points $\mathbf{r}_2$ around the macromolecule. If an ordinary rectangular grid of $N \times N \times N$ nodes is used for numerical solution of eq 5, then the number of resulting eqs 3.2 is about $N^3$. Equation 5 is quite similar to the PB equation for which $N$ should be within 50−100 for the model of a globular protein. On the other hand, eq 3 is similar to the linear PB equation, and one has to use the grid of comparative dimension to solve it. It is clear that $50^3$ boundary problems within one cycle (5)−(3)−(1)−(5) is too difficult a task even for modern supercomputers, and the choice of nonuniform grid of points $\mathbf{r}_2$ becomes crucial. The last yields the problem of interpolation of a function distributed on the nonuniform three-dimensional net of points and the problem of choice of paths for integration of eq 2.

All of the problems outlined above were successfully solved within the framework of the finite-difference (FD) method applied to eqs 3 and 5. To avoid the mentioned singularity, the fluctuation potential and the $\eta$ function from eq 2 are expressed as sums of two terms corresponding to the two terms of the right-hand side of eq 3.2: $\phi_\alpha(\mathbf{r}_1,\mathbf{r}_2) = \phi_\alpha{}^\psi(\mathbf{r}_1,\mathbf{r}_2) + \phi_\alpha{}^\delta(\mathbf{r}_1,\mathbf{r}_2)$ and $\eta_\alpha(\mathbf{r}) = \eta_\alpha{}^\psi(\mathbf{r}) + \eta_\alpha{}^\delta(\mathbf{r})$. This leads to two seaprate problems 3 for $\phi_\alpha{}^\psi$ and $\phi_\alpha{}^\delta$ and two eqs 2 for $\eta_\alpha{}^\psi$ and $\eta_\alpha{}^\delta$. Problem 3 for $\phi_\alpha{}^\psi$ does not involve a singularity at all. For $\eta_\alpha{}^\delta$, using symmetry of the $\phi_\alpha{}^\delta(\mathbf{r}_1,\mathbf{r}_2)$ with respect to $\mathbf{r}_1$ and $\mathbf{r}_2$, we obtain an analytical solution of eq 2:

$$\eta_\alpha{}^\delta(\mathbf{r}_2) = \frac{1}{2}\lim_{\mathbf{r}_1\to\mathbf{r}_2}[\phi_\alpha{}^\delta(\mathbf{r}_1,\mathbf{r}_2) - u_\alpha(r_{12})]$$

This solution has a simple numerical implementation. As in the previous paper,[27] no charge distribution for the $\delta$-function in eq 3.2 is used. The "point charge" is assigned to a lattice mode. The resulting magnitude of $\phi_\alpha{}^\delta(\mathbf{r}_2,\mathbf{r}_2)$ is completely dependent on the grid spacing, but, as follows from numerous tests, any difference $\phi_\alpha{}^\delta(\mathbf{r},\mathbf{r}) - \phi_\alpha{}^\delta(\mathbf{r}',\mathbf{r}')$ depends only on boundary conditions and the "singularity" is subtracted. Finally we obtain

$$\eta_\alpha{}^\delta(\mathbf{r}) - \eta_\alpha{}^\delta(\infty) \approx \frac{1}{2}[\phi_\alpha{}^\delta(\mathbf{r},\mathbf{r}) - \phi_\alpha{}^\delta(\infty)]$$

The nonuniform net of the $\delta$-function positions from eq 3 is a crucial point of the algorithm. The following method was used. The macromolecule together with the zone of exclusion of ions is surrounded by three layers of points $\mathbf{r}_2$ from eq 3.2. The first, most internal layer has a thickness half the Debye−Huckel length $\lambda_{DH}$ for the bulk electrolyte. The others are of thickness $\lambda_{DH}$. Every point of the grid of FD solution of eq 5 is taken as a point $\mathbf{r}_2$ for eq 3 within the first layer. The nodes of the grid for eq 5 are also taken as points $\mathbf{r}_2$ within other layers, but spacing between them is doubled for the second layer and 4 times higher for the third one. The rest of external part of the grid for eq 5 is distributed by positions of the $\delta$-function with 8 times higher spacing. The described method of distributing $\mathbf{r}_2$ points allows a number of them to be radically reduced. If the main grid of eq 5 has dimension of $60 \times 60 \times 60$, then the corresponding number of eqs 3 appears to be within 8000−12 000 under conditions that the length of the grid is the sum of molecule's size and six $\lambda_{DH}$. Such an amount of computations can be practically done in a reasonable time. It should be noted that the biggest part of the calculations originates from the first internal layer of the singularity points. As follows from tests, its replacement by extension of the computationally much cheaper second layer notably spoils the results, although the choice of its thickness does not affect them starting from the value of $\lambda_{DH}/2$.

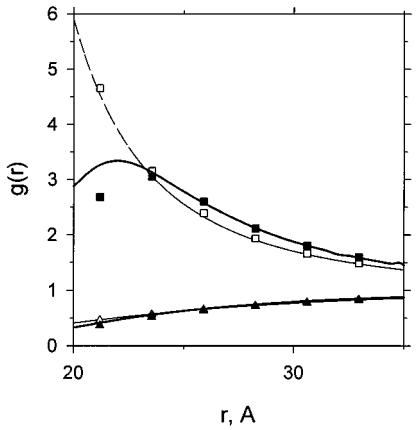


**Figure 1.** Ionic distribution functions around a uniformly charged sphere of 18 Å radius and charge $+7e$. Internal permittivity $\epsilon = 10$, solvent permittivity $\epsilon_w = 80$, 1:2 RPM electrolyte, ionic diameter is 4 Å, $C_{Salt} = 0.0167$ M; the solid curves are 1D solutions of the BBGY equations; the dashed curves are 1D solutions of the PB equation; open and filled triangles and squares are data of corresponding 3D solutions.

For eq 5 the same numerical implementation is used as described for FD solution of the similar PB equation in refs 1 and 5. Equation 3 is linear, which simplifies the problem of convergence.[29]

The macromolecule is described in terms of its three-dimensional structure as determined by the coordinates of its atoms. The atomic coordinates are taken from the Brookhaven Protein Data Bank (PDB).[30] Because of the relatively high value of the ion exclusion radius (see below), the charges are assigned only to the ionized groups of the protein and no other partial charges are considered.

The evaluation of the transfer free energy (eq 9) requires several solutions of the BBGY equations in order to obtain the charging integral (eq 7). Fortunately, as follows from tests, only a few (3−5) such solutions are actually needed. The solution at $\lambda = 0$ is also applied to integral 8.

## 4. Test of Accuracy

The algorithm was programmed and tested on the model of a uniformly charged sphere where one-dimensional (1D) Runge−Kutta solutions of eq 5 can be combined with three-dimensional (3D) solutions of eq 3 similarly as in cylindrical geometry applications described in the previous work.[27] The uniformly charged sphere of 18 Å radius, internal dielectric constant $\epsilon = 2$, 10, and 80, and $+7e$ charge was taken as an example. The permittivity of surrounding solvent $\epsilon_w$ was set to 80. The one-dimensional solution was tested for the constant coefficient $k^2(\mathbf{r}_1) \equiv K^2$, where an analytical solution of eq 3 can be obtained. As in the previous work, such a comparison has shown that errors of the $\eta$ function evaluation are within a few percent even if the strongest dielectric discontinuity ($\epsilon = 2$, $\epsilon_w = 80$) is present in the model. Comparison of 3D solutions with corresponding 1D solutions for the sphere is shown in Figures 1−4. The calculations were performed for several

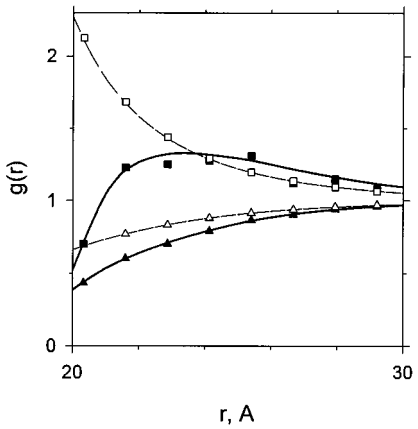


**Figure 2.** The same data as in Figure 1 for $C_{Salt} = 0.167$ M ($I = 1.0$ M); symbols as given in Figure 1.

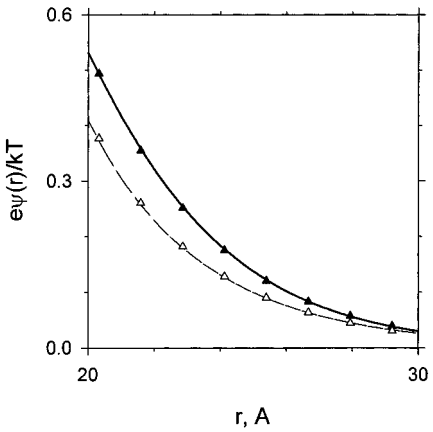


**Figure 3.** Mean electrostatic potential for a model from Figure 2; notation as given in Figure 1.

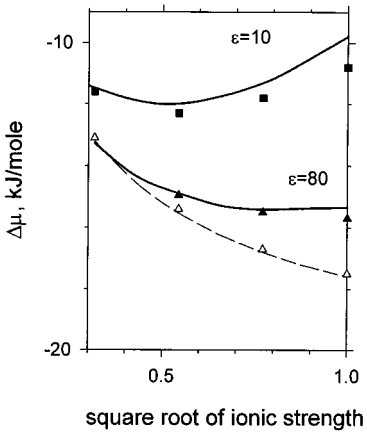


**Figure 4.** Comparison of 1D and 3D $\Delta\mu$ calculations as a function of 1:2 salt concentration for the model from Figures 1−3 taken at two different $\epsilon$: $\epsilon = 10$ and $\epsilon = \epsilon_w = 80$; both PB curves are identical; notation as in Figure 1.

concentrations of 1:1 and 1:2 salts related to ionic strengths from 0.32 to 1.0 M. The last value is the upper limit for all applications described in this paper. The ionic radius was taken as 2.0 Å. The sizes of the lattice to solve eqs 3 and 5 were determined as a sum of the macromolecule's sizes (diameter of the sphere), ion exclusion diameter, and six Debye−Huckel lengths for the bulk electrolyte. The $75 \times 61 \times 61$ lattice was used to solve eq 3 in the case of 1D geometry. The lattice spacing is varied from 2.04 Å ($I = 0.32$ M, $\lambda_{DH} = 13.7$ Å) to 1.1 Å ($I = 1.0$ M, $\lambda_{DH} = 4.3$ Å). In the case of the 3D solutions, the lattice is not so thick and includes $53^3$ nodes. The corresponding lattice spacing is varied from 2.3 to 1.3 Å. The amount of computational work is very large in the case of the 3D algorithm. The number of points $\mathbf{r}_2$ (i.e., the number of eqs 3 involved into the main loop (5)−(3)−(1)−(5)) is approximately from 7000 for $I = 0.32$ M to 10 000 for $I = 1$ M. In the case of 1D solutions, there are only about 30 such points lying on the radial line outside the sphere.

The convergence of the iteration process (5)−(3)−(1), etc., was very fast: it was obtained after 2−3 loops. The accuracy of numerical 3D solutions of eq 5 was also checked by evaluation of the total ionic charge around the sphere. It should be of opposite sign and equal magnitude as the charge of the sphere, providing the neutrality of the system. For the grid of dimension $53^3$, the relative errors appear to be within 2%. Such errors are negligible in the case of 1D solution.

In Figures 1−4 only the data for the 1:2 salt are presented (counterions are divalent). The comparison for the 1:1 salt shows a good agreement between the PB and BBGY results because of weakness of the repulsive image forces acting on monovalent ions. In the case of multivalent electrolyte, one can see such features of the BBGY curves as the exclusion of ions due to electrostatic imaging in the vicinity of the sphere and a resulting horizontal shift of curves at higher distances caused by increase of the "effective radius" of the macroion.[27] Although the discrepancy does not seem to be too high, it drastically affects the macroion's transfer free energy dependence 9, as it is seen from comparison given in Figure 4. At ionic strength $I = 1.0$ M ($C_{1:2} = 0.167$ M), one can observe a difference up to 2 times between $\Delta\mu_{PB}(C_{Salt})$ and $\Delta\mu_{BBGY}(C_{Salt})$.

We can say that long-range Coulombic forces are responsible, at least in part, for the increase of the macromolecule's free energy with increase of salt concentration, an effect known as salting-out. Its explanation was given many decades ago.[31] The effect is caused by electrostatic repulsion of ions from a cavity of low-dielectric medium, representing a macromolecule. This repulsion is positive work against osmotic pressure of the ionic gas. It is important to note that the PB equation cannot describe the salting-out effect in principle. Regardless of parametrization, the PB electrostatic energy of the system is always monotonically decreased with an increase in ionic concentration because of growing charge screening.

The test has also demonstrated the possibility of applying the BBGY equations to a realistic model of the macromolecule, as was previously done for the PB equation.[1] In Figures 1−4 one can see a very good agreement between one-dimensional solutions of eq 5 and solutions produced by a computer program designed for arbitrarily complex macromolecules.

## 5. Results and Discussion

The three-dimensional structure of the hen egg lysozyme molecule (PDB entry 2LYZ)[32] was taken for comparison of PB with BBGY calculations. Ionizable groups of atoms were assigned to be charged (Arg +1, Lys +1, Asp −1, Glu −1, His +0.5, C terminus −1), which leads to a total charge of $+7.5e$. No other partial charges of atoms were considered. The model approximately describes a charged state of the protein at pH ≈ 8.[33] Although such description of the protein's charges is apparently rough, it may be applied to calculation of the difference between $\Delta\mu_{BBGY}$ and $\Delta\mu_{PB}$ as it is caused only by the corresponding difference of mobile ion distributions. (For example, such a model of charges cannot be used for calculations of p$K$'s of charged groups.) The internal permittivity of the molecule was set to 12 (also 80), the solvent permittivity was 80. The thickness of the shell of ionic exclusion around the macromolecule and radius of exclusion for ion−ion interactions were considered as two independent parameters.

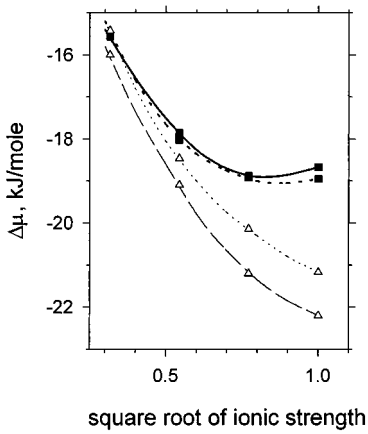


**Figure 5.** Transfer free energy for the lysozyme molecule; 1:2 electrolyte, $\epsilon_w = 80$. The dashed and solid curves are the PB and BBGY results, respectively, at $\epsilon = 12$; the thin and thick dotted curves correspond to the PB and BBGY results at $\epsilon = \epsilon_w = 80$.

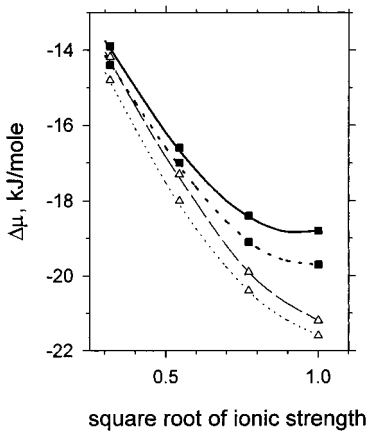


**Figure 6.** Transfer free energy for the lysozyme molecule; 2:1 and 1:1 electrolytes; $\epsilon = 12$; $\epsilon_w = 80$. The dashed and solid curves correspond to the PB and BBGY results for 2:1 electrolyte; the thin and thick dotted curves correspond to the PB and BBGY results for 1:1 electrolyte.

This requires some comments. It is known that one may apply Coulombic interactions with macroscopic permittivity of water only beyond the first few angstroms from atoms of the macromolecule.[19] The continuum model is inadequate within a thin layer surrounding the water accessible surface. For example, as follows from data of molecular dynamics simulations for ions,[34,35] interactions between two ions obey the Coulombic law only if at least one water molecule can be placed between them. At shorter distances strong polarization forces immediately act on ions from water molecules. They always pull the ions away from each other and essentially exceed the Coulombic attraction of ions. The same kind of forces must affect ions in the vicinity of the macromolecule's atoms, repelling ions from the surface of the macromolecule. Such a picture was observed in results of Monte Carlo simulations with SPC water on the counterion distribution in regions close to a highly charged polyelectrolyte.[36] In the case of the explicit solvent model, the counterions were found to avoid regions near the polyion. We may assume that a similar picture can be observed for any charged macromolecule. It may lead to an increase of the "effective" radius of short-range ion−macromolecule repulsion in comparison with the radius of exclusion of ions for the bulk electrolyte. On the other hand, this "effective" radius of ionic exclusion should not be much higher than the sum of the van der Waals radius of an ion and the water molecule diameter, i.e., about 4−4.5 Å. As a result, we have to apply it as an independent parameter of our model. The value of 3.5 Å was used (also 2 Å for comparison), whereas the hard sphere radius for ion−ion interactions was fixed at 2 Å.

The three-dimensional solution of the system of eqs 1−5 was obtained for the lysozyme molecule. The salt dependencies of $\Delta\mu_{PB}$ and $\Delta\mu_{BBGY}$ were calculated for 1:2, 2:1, and 1:1 electrolytes in the range of ionic strengths from 0.32 to 1.0 M. The dimension of the grid for eq 5 was taken as $53 \times 49 \times 53$ at $I = 0.32$ M to $53 \times 49 \times 57$ (also $61 \times 57 \times 65$ for comparison) at $I = 1.0$ M. The corresponding grid spacing is varied from 2.5 Å at $I = 0.32$ M to 1.4 Å (1.3 Å) at $I = 1.0$ M. The number of eqs 3 varies from 7650 to 9750 (12 500), respectively. The results are shown in Figures 5 and 6. As we can see, the ion finite size effects have only a weak influence on the resulting curves. Although the difference between $\Delta\mu_{BBGY}$ and $\Delta\mu_{PB}$ is notable and reaches ~1 kcal/mol for a 1:2 electrolyte at $I = 1.0$ M ($C = 0.167$ M), it is much less than the main term due to the charge screening ($\Delta\mu_{PB}(0.167\text{ M}) = -5.3$ kcal/mol). In fact there is no difference between the PB and BBGY mean electrostatic potentials of the protein's charges. Even for a 1:2 salt at $I = 1.0$ M, the integral $^1/_2\int\rho_0(\psi_{BBGY} - \psi_{PB})d^3\mathbf{r}$ is about −0.3 kJ/mol, which is a negligibly small value. The last explains the success of numerous applications of the PB equation to calculations of p$K_a$'s of ionizable groups in proteins[3,8,33,37,38] even in the case of high concentrations of electrolyte. It should be noted that a drop of $\Psi_{BBGY}(\mathbf{r})$ is faster than that of $\Psi_{PB}(\mathbf{r})$ far from the macromolecule, and the difference between $\Psi_{BBGY}(\mathbf{r})$ and $\Psi_{PB}(\mathbf{r})$ grows and becomes significant (up to 50% in the case of a 1:2 electrolyte) at distances of several angstrom units from the macromolecule's surface. The influence of internal dielectric properties on resulting curves is surprisingly small. As follows from comparison of data represented in Figure 5, about half of the discrepancy between $\Delta\mu_{PB}$ and $\Delta\mu_{BBGY}$ comes from the dielectric discontinuity, but a change of $\Delta\mu_{PB}$ together with a change of $\epsilon$ compensates the effect. As a result, curves of $\Delta\mu_{BBGY}$ at $\epsilon = 12$ and of $\Delta\mu_{BBGY}$ at $\epsilon = \epsilon_W = 80$ are almost identical.

A choice of the "effective" radius of ion−macromolecule repulsive interactions weakly affects $\Delta\mu$. The difference $\Delta\mu_{BGGY} - \Delta\mu_{PB}$ is about 30% higher if a value of 2 Å is taken instead of 3.5 Å (data not shown). The last suggests that this unknown parameter is not critical and may be set arbitrarily within the range chosen.

The correctness of the calculations described above was checked by an increase of the grid dimension (decrease of the grid spacing), changing configurations of layers of singularity positions, and an increase of a number of charging states in the charging integral (9). All the experiments have shown an excellent stability of the results. For example, doubling of the thickness of the internal layer of points $\mathbf{r}_2$ from eq 3 changes the difference between $\Delta\mu_{BBGY}$ and $\Delta\mu_{PB}$ within a few percent of its value obtained with the adopted thickness of $\lambda_{DH}/2$. An external charge of the ionic cloud around the macromolecule was in agreement with the value of the macromolecule's charge within an accuracy of 1−2%.

As we can see, the image forces and interionic correlations have a relatively weak effect on the thermodynamics of lysozyme at least at moderately low salt concentrations. This result can be explained via a high electrostatic field near the macromolecule's surface. The test model of a uniformly charged sphere described in the previous section was close to the "spherical approximation" of the lysozyme molecule, and Figure 5 was expected to be similar to Figure 4. It is clear

now that nonuniform charge distribution together with essentially a higher absolute value of the total charge has reduced the difference between $\Delta\mu_{BBGY}$ and $\Delta\mu_{PB}$ in the case of the more realistic model of the macromolecule. We can assume that the difference would be higher for a larger and weakly charged protein molecule. The difference between PB and BBGY results might be significant for the highly charged molecule of DNA in the case of multivalent electrolyte.[27]

The results of calculations do not show a significant salting-out effect for lysozyme, which is in strong contradiction with experimental data. The value of $\partial\Delta\mu/\partial C_{Salt}$ was measured for hen egg lysozyme in various electrolyte solutions.[16−18] All the data for multivalent salts were measured at concentrations where the continuum dielectric model is inadequate. For a 1:1 electrolyte (NaCl) data are available at $C_{Salt} = 0.5$ M ($I = 1.0$ M) and can be used for comparison with the BBGY results. The experimental value of the derivative[17] is +6.3 (±1.0) kcal/mol of protein/mol of salt at pH = 7.0, indicating a very rapid growth of the free energy of lysozyme with an increase of salt concentrations. Looking at Figure 6, one can see that the part of the $\partial\Delta\mu/\partial C_{Salt}$ related to long-range electrostatics is close to zero. There is a very simple explanation for this fact. In eq 9 of the free energy dependence on salt concentration we omitted the term for the short-range exclusion of ions from the macromolecule's surface. As mentioned above, these forces cannot be described within the framework of Coulombic electrostatics and require microscopic description. They obviously depend on the kind of ions, the macromolecule's shape, and the charge distribution. Despite the mentioned complex nature of these polarization forces, in one instance they are simpler than the long-range electrostatics. At low ionic concentrations their part of the free energy dependence $\Delta\mu(C_{Salt})$ should be strictly proportional to the salt concentration:

$$\Delta\mu(C_{Salt}) = \lambda C_{Salt} + W_0(C_{Salt}) + W_{Ch}(C_{Salt}) - W_{Ch}(0) \quad (10)$$

This new term of the free energy appears via the positive work of ionic gas pressing within the thin shell of ionic exclusion and can be very roughly estimated by $\lambda C_{Salt} = n_{ions}kTS_{Acc}(\mathbf{r}_{ion\text{-}m} - \mathbf{r}_w)$, where $n_{ions}kT$ is the osmotic pressure of the ionic gas, $S_{Acc}$ is the accessible surface area of a macromolecule, $\mathbf{r}_{ion\text{-}m}$ is the radius of exclusion of ions adopted for macromolecule−ion interactions (3.5 Å for our model), and $r_w$ is the van der Waals radius of the water molecule (1.4 Å). The value of accessible surface area of the lysozyme molecule is 6700 Å$^2$, and an estimated value of $\partial\Delta\mu/\partial C_{Salt}$ for a 0.5 M solution of a 1:1 electrolyte is about +10 kcal/mol of protein/mol of salt. Despite an agreement with experimental data, this estimation should not be considered as an attempt to obtain this value from the first principles; it is rather a justification of the choice of $\mathbf{r}_{ion\text{-}m} = 3.5$ Å. Actually, to extract the true $\Delta\mu(C_{Salt})$ for the lysozyme, we need to take this term from experimental data. The resulting curve is shown in Figure 7 and demonstrates that the PB equation should not be applied to the free energy dependence of ionic concentration if access of ions to the surface of the molecule is changed during the process considered. In other words, despite correct calculations of the electrostatic energy of ionizable groups, the PB equation cannot be applied to studies of salt dependence of processes involving aggregation of macromolecules.

## 6. Conclusions

The comparison of $\partial\Delta\mu_{BBGY}/\partial C_{1:1}$ with experimental data (see $\partial\mu_2/\partial m_3$ column in Table V of ref 17) reveals the great influence of the first coordination shell of the solvent molecules on the thermodynamics of macromolecules in electrolyte solutions. There is no doubt that the BBGY equations together with the continuum solvent model are a correct description of long-range electrostatics at salt concentrations used in the present work. Even at $C_{1:1} = 0.5$ M the mean distance between ions is higher than 10 Å both in the bulk electrolyte and in the areas of ionic excess around the protein molecule, which makes the application of the Coulombic law with macroscopic permittivity possible. The discrepancy with experimental data can only originate from the vicinity of the macromolecule. The effect of ionic exclusion from the first coordination shell of water molecules has been described in the literature through the years. It was used not merely for explanation of thermodynamics of protein solubility (see, for example, ref 18) but also in interfacial electrochemistry, where exclusion of ions from the monomolecular inner layer of the electrical double layer was necessary for fitting of the differential capacitance of the electrolyte.[39] The existence of this excluded volume is confirmed by experimental data of water surface tension dependencies on salt concentration.[40] For 1 M NaCl the value of $\partial\sigma/\partial C_{Salt}$ is 1.64 dynes per centimeter per mole of salt, which immediately leads to the similar thickness of exclusion zone about 3 Å (when neglecting long-range electrostatics). Detailed MD simulations of the potential of mean force acting on mobile ions in the vicinity of a macromolecule's surface will allow the quantification of the above-mentioned effect.

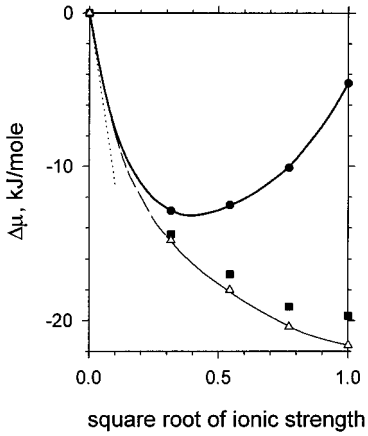


**Figure 7.** Explanation for salting-out of the lysozyme for 1:1 electrolyte. The triangles and squares represent data shown as dotted curves in Figure 6; the circles and solid curve represent the true curve of $\Delta\mu(C_{1:1})$ (eq 10) with the $\lambda C_{1:1}$ term taken from experimental data. The dotted line is the Debye−Huckel limit at infinite dilution of electrolyte.

We conclude that the PB equation can be applied to calculations of the electrostatic energy of proteins' ionizable groups even at high ionic concentrations. In contrast, the PB calculations of various phase transition free energies (i.e., transfer between two media, protein crystallization, precipitation, and so on) should be restrained to extremely diluted solutions of electrolytes.

**Acknowledgment.** The calculations presented in this paper were in part executed thanks to the computational grant at the Interdisciplinary Modelling Center of Warsaw University.

## References and Notes

(1) Klapper, I.; Hagstrom, R.; Fine, R.; Sharp, K.; Honig, B. *Proteins* **1986**, *1*, 47.
(2) Vorobjev, Y. N.; Grant, J. A.; Scheraga, H. A. *J. Am. Chem. Soc.* **1992**, *114*, 3189.
(3) Luty, B. A.; Davis, M. E.; McCammon, J. A. *J. Comput. Chem.* **1992**, *13*, 1114.
(4) Oberoi, H.; Allewell, N. M. *Biophys. J.* **1993**, *65*, 48.

(5) Jayaram, B.; Sharp, K. A.; Honig, B. *Biopolymers* **1989**, *28*, 975.
(6) Sharp, K. A.; Honig, B. *J. Phys. Chem.* **1990**, *94*, 7684.
(7) Zhou, H. *J. Chem. Phys.* **1994**, *100*, 3152.
(8) Bashford, D.; Karplus, M. *Biochemistry* **1990**, *29*, 10219.
(9) Sharp, K. A. *Biopolymers* **1995**, *36*, 245.
(10) Carnie, S. L.; Torrie, G. M. *Adv. Chem. Phys.* **1984**, *56*, 141.
(11) Murthy, C. S.; Bacquet, R. J.; Rossky, P. J. *J. Phys. Chem.* **1985**, *89*, 701.
(12) Mills, P.; Anderson, C. F.; Record, M. T., Jr. *J. Phys. Chem.* **1985**, *89*, 3984.
(13) Degreve, L.; Lozada-Cassou, M. *Mol. Phys.* **1995**, *86*, 759.
(14) Lamm, G.; Wong, L.; Pack, G. R. *Biopolymers* **1994**, *34*, 227.
(15) Arakawa, T.; Timasheff, S. N. *Methods Enzymol.* **1985**, *114*, 49.
(16) Arakawa, T.; Timasheff, S. N. *Biochemistry* **1984**, *23*, 5912.
(17) Arakawa, T.; Timasheff, S. N. *Biochemistry* **1987**, *26*, 5147.
(18) Arakawa, T.; Bhat, R.; Timasheff, S. N. *Biochemistry* **1990**, *29*, 1914.
(19) Torrie, G. M.; Patey, G. N. *J. Phys. Chem.* **1993**, *97*, 12909.
(20) Tang, Z.; Scriven, L. E.; Davis, H. T. *J. Chem. Phys.* **1992**, *97*, 494.
(21) Lamperski, S.; Outhwaite, C. W.; Bhuiyan, L. B. *Mol. Phys.* **1996**, *87*, 1049.
(22) Levine, S.; Bell, G. M. *J. Phys. Chem.* **1960**, *64*, 1188.
(23) Levine, S.; Outhwaite, C. W. *J. Chem. Soc., Faraday Trans. 2* **1978**, *74*, 1670.
(24) Outhwaite, C. W.; Bhuiyan, L. B. *Mol. Phys.* **1991**, *74*, 367.
(25) Outhwaite, C. W. *J. Chem. Soc., Faraday Trans. 2* **1986**, *82*, 789.
(26) Outhwaite, C. W. *J. Chem. Soc., Faraday Trans. 2* **1978**, *74*, 1214.
(27) Gavryushov, S.; Zielenkiewicz, P. *J. Phys. Chem. B* **1997**, *101*, 792.
(28) Bell, G. M.; Levine, S. In *Chemical Physics of Ionic Solutions*; Conway, B. E., Barradas, R. G., Eds.; Wiley: New York, 1966.
(29) Nicholls, A.; Honig, B. *J. Comput. Chem.* **1991**, *12*, 435.
(30) Bernstein, F. C.; Koetzle, T. F.; Williams, G. J. B.; Meyer, E. F., Jr.; Brice, M. D.; Rodgers, J. R.; Kennard, O.; Shimanouchi, T.; Tasumi, M. *J. Mol. Biol.* **1977**, *112*, 535.
(31) Kirkwood, J. G. In *Proteins, Amino Acids and Peptides*; Cohn, E. J., Edsall, J. T., Eds.; Van Nostrand-Reinhold: Princeton, NJ, 1943; p 276.
(32) Diamond, R. *J. Mol. Biol.* **1974**, *82*, 371.
(33) Schaefer, M.; Sommer, M.; Karplus, M. *J. Phys. Chem. B* **1997**, *101*, 1663.
(34) Zhu, S. B.; Robinson, G. W. *J. Chem. Phys.* **1992**, *97*, 4336.
(35) Smith, D. E.; Dang, L. X. *J. Chem. Phys.* **1994**, *100*, 3757.
(36) Gordon, H. L.; Goldman, S. *J. Phys. Chem.* **1992**, *96*, 1921.
(37) Takahashi, T.; Nakamura, H.; Wada, A. *Biopolymers* **1992**, *32*, 897.
(38) Loewenthal, R.; Sancho, J.; Reinikainen, T.; Fersht, A. R. *J. Mol. Biol.* **1993**, *232*, 574.
(39) Macdonald, J. R.; Barlow, C. A., Jr. *J. Chem. Phys.* **1962**, *36*, 3062.
(40) Arakawa, T.; Timasheff, S. N. *Biochemistry* **1982**, *21*, 6545.